Injury, Int. J. Care Injured (2004) **35**, S-A105—S-A112

ELSEVIER

INJURY
INTERNATIONAL JOURNAL OF THE CARE OF THE INJURED

www.elsevier.com/locate/injury

New method to assess the registration of CT-MR images of the head

Ion P. Pappas[1], Malik Puja[1], Martin Styner[1], Jubei Liu[1], Marco Caversaccio[2]

[1] *M.E.Müller Research Center, University of Bern, 3001 Bern, Switzerland*
[2] *Inselspital, ORL-Department, University of Bern, 3010 Bern, Switzerland*

KEYWORDS:
CT; MR; fusion;
registration;
assessment.

Summary[1] Due to their complementary information content, both x-ray computed tomography (CT) and magnetic resonance (MR) imaging are employed in certain clinical cases to improve the understanding of pathology involved. o spatially relate the two datasets, image registration and image fusion are employed. However, registration errors, either global or local, are common and are non-uniform within the image volume. In this paper, we propose a new algorithm that assesses the quality of the registration locally within the CT-MR volume and provides visual, color-coded feedback to the user about the location and extent of good and bad correspondence between the two images.
The proposed registration assessment algorithm is based on a correspondence analysis of bone structures in the CT and MR images. For that purpose, a custom segmentation algorithm for bone in MR images has been developed that is based on a stochastic threshold computation method. This segmentation method for MR images and the CT-MR registration assessment algorithm were validated on simulated MR datasets and real CT-MR image pairs of the head. Some partial-volume effects occur at the borders of the bone structures and at the bone interfaces with air, which cannot be separated from bone in the MR image.
The presented assessment method of CT-MR image registration offers the user a new tool to evaluate the overall and local quality of the registration. With this information, the user does not have to blindly trust the fused CT-MR datasets but can easily identify areas of inaccurate correspondence. The application of the algorithm is so far limited to T1-weighted MR and CT images of the head area.

Introduction

Preamble

X-ray computed tomography (CT) and magnetic resonance tomography (MR) are two imaging modalities that have been widely used in medicine since the 1980s to visualize the interior of the human body and in particular the interior of the head. These two modalities are based on different physical principles and lead to images of very different informational content. X-ray tomography offers high contrast in visualization of bone structures, but soft tissue contrast is poor. Conversely, MR imaging offers high contrast for the visualization of the soft-tissue morphology (cerebral gray and white matter, blood vessels) but produces a weak signal in bone. Due to the complementary nature of the two imaging modalities, in certain cases patients are imaged with

[1] Abstracts in German, French, Italian, Spanish, Japanese, and Russian are printed at the end of this supplement.

0020–1383/$ — see front matter
doi:10.1016/j.injury.2004.05.018

both CT and MR. In order to spatially relate the two sources of information, the data are registered, ie, brought to spatial alignment, and usually fused into a common display.

Fused representations of CT-MR images of the head are valuable in the field of ENT, CMF and neurosurgery for diagnosis, surgical planning, and during image-guided interventions. They provide improved understanding of the relationship between soft tissue and bone. For example, fused CT-MR images improve the ability of the user to identify the limits of a tumor. The CT provides information on the extent of bone erosion, while the MR shows the extent of brain invasion. This combined imaging can lead to more precise resection or treatment of tumors, better positioning of craniotomies, and reduced craniotomy size. Fused representations of CT and MR images can be viewed in a variety of ways: as color overlays, as segmented bone or bone contours extracted from the CT overlaid on the MR, or as a weighted average of corresponding pixels with normalized intensity gray values (color images available upon request).

Performing the registration of two image volumes of different modalities such as CT and MR used to be a challenging mathematical task. First efforts were based on the so-called 'pair-point registration', a manual identification of a number of homologous anatomical points in the two volumes. In the mean time, a variety of automatic registration methods [13] have been proposed including methods using stereotactic frames, surface measurements, segmented objects, and methods that directly use directly the gray value intensities such as the widely used mutual information algorithms [4—5]. Today, rigid co-registration (six degrees of freedom) of standard CT-MR image pairs of the head can be completed within minutes or seconds.

Technical issues

To achieve a successful multimodal registration, all algorithms have to deal with the following technical issues [6].

The two image volumes do not usually cover exactly the same portion of the targeted anatomical area. Due to the risk associated with the x-ray exposure in CT, it is common for the CT image to have a much smaller field of view than the corresponding MR image. Furthermore, the in-slice and through-slice spatial resolution of the two image volumes is different. Commonly, CT images contain 512x512 pixels in each slice, while the image matrix in MR usually has 256x256 pixels. For the resolution in the through-slice direction, the situation is usually the opposite. To reduce the radiation exposure, fewer and thicker slices are often used in CT than in MR. These differences have important consequences for CT-MR registration and the algorithms needed to correctly deal with them. For the visualization of both data in a common display and to avoid loss of resolution, the data have to be resampled in a new volume that has higher resolution than either of the initial volumes.

Another very important issue in image registration is image distortion. MR acquisition is affected by distortions due to inhomogenies in the static magnetic field or due to distortions of the magnetic field generated by the different magnetic susceptibility properties of different materials (chemical shift artifacts), such as soft tissue and air [7]. In the area of the head, these distortions are important around the frontal, maxillary, and sphenoid sinuses. The physics of CT acquisition are practically free of such distortion effects per se. However, errors in the calibration of the bed speed or the gantry tilt can lead to substantial distortions of the real anatomy with up to a few millimeters of total error. These distortions can become quite apparent in registered images.

Motivation

Although some existing automatic registration algorithms have been shown in controlled experiments to achieve high registration accuracy for CT-MR datasets [3], the accuracy is different for every new CT-MR pair, and even the best algorithms can sometimes fail, leading to errors that can be as large as 6 mm or more [2]. Furthermore, even when the global registration is good, image distortion effects lead to local target registration errors. Last but not least, in spite of the currently available automatic registration algorithms, image alignment is still commonly performed manually with visual inspection, or using anatomical pair-points, which is error prone and time consuming. Moreover, it has been shown that even experienced observers cannot reliably detect visually misregistrations of less than 2 mm [8]. Due to the above-mentioned sources of registration errors, a complete 3-dimensional assessment of the registration accuracy would be desirable before the registered or fused image pair is used clinically [9].

In the following section, we present an automatic, local registration assessment algorithm for CT and MR images of the head, which classifies individual voxels as 'well-registered' or 'badly-registered', based on a correspondence analysis of individual voxels of bone structures in CT and MR datasets. The result of this assessment algorithm is color-coded and visualized in

a fused CT-MR image volume. This process makes it easy for the human operator to identify the regions of low and high registration accuracy.

Methods

Registration assessment algorithm

The proposed registration assessment method for CT-MR images of the head is based on a correspondence analysis of the bone structures. In CT images, dense structures such as bones are imaged with high signal intensity due to their strong absorption of x-rays, whereas in MR images the signal intensity of dense structures is low due to their low content of excitable hydrogen atoms. The registration assessment method is summarized by the following steps and illustrated by Figure 2a—f.

The CT and MR datasets (Fig. 2a, b) are registered and resampled to obtain a voxel-by-voxel correspondence.

Bone structures in the CT image are segmented using a user-adjustable threshold, initialized based on

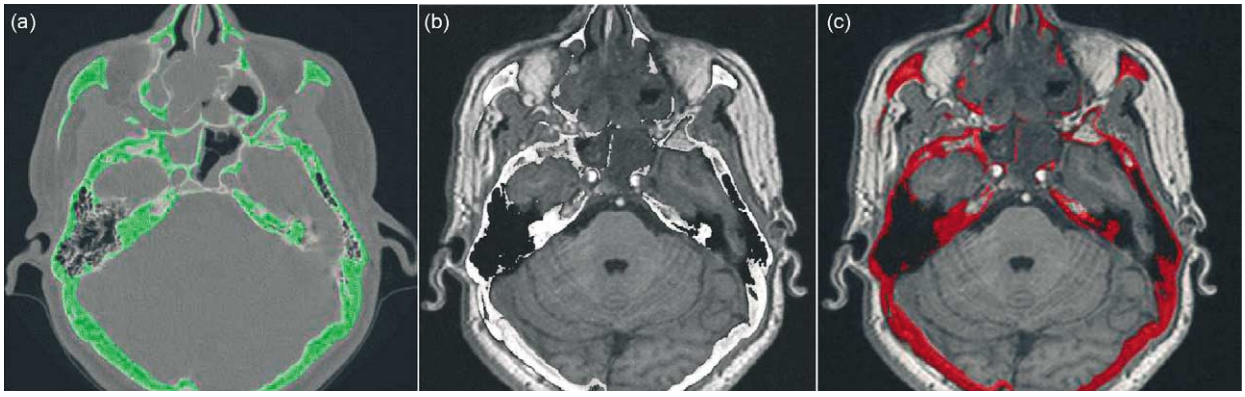

Fig. 1a: CT image with segmented bone colored in green. b) Fused CT-MR dataset, where the segmented bone from the CT has been overlaid after adjustment of the intensity values on the MR. c) Segmented bone from CT overlaid in red color on the MR image.

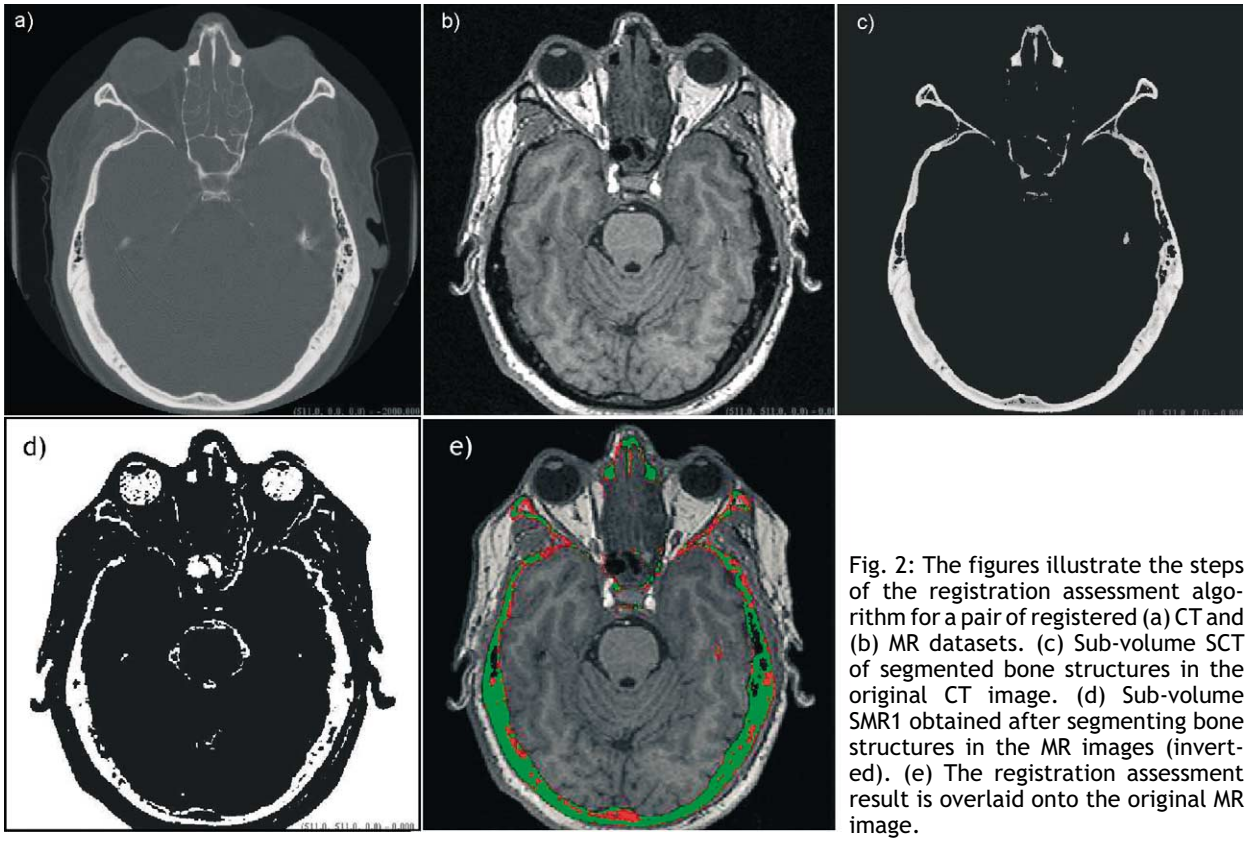

Fig. 2: The figures illustrate the steps of the registration assessment algorithm for a pair of registered (a) CT and (b) MR datasets. (c) Sub-volume SCT of segmented bone structures in the original CT image. (d) Sub-volume SMR1 obtained after segmenting bone structures in the MR images (inverted). (e) The registration assessment result is overlaid onto the original MR image.

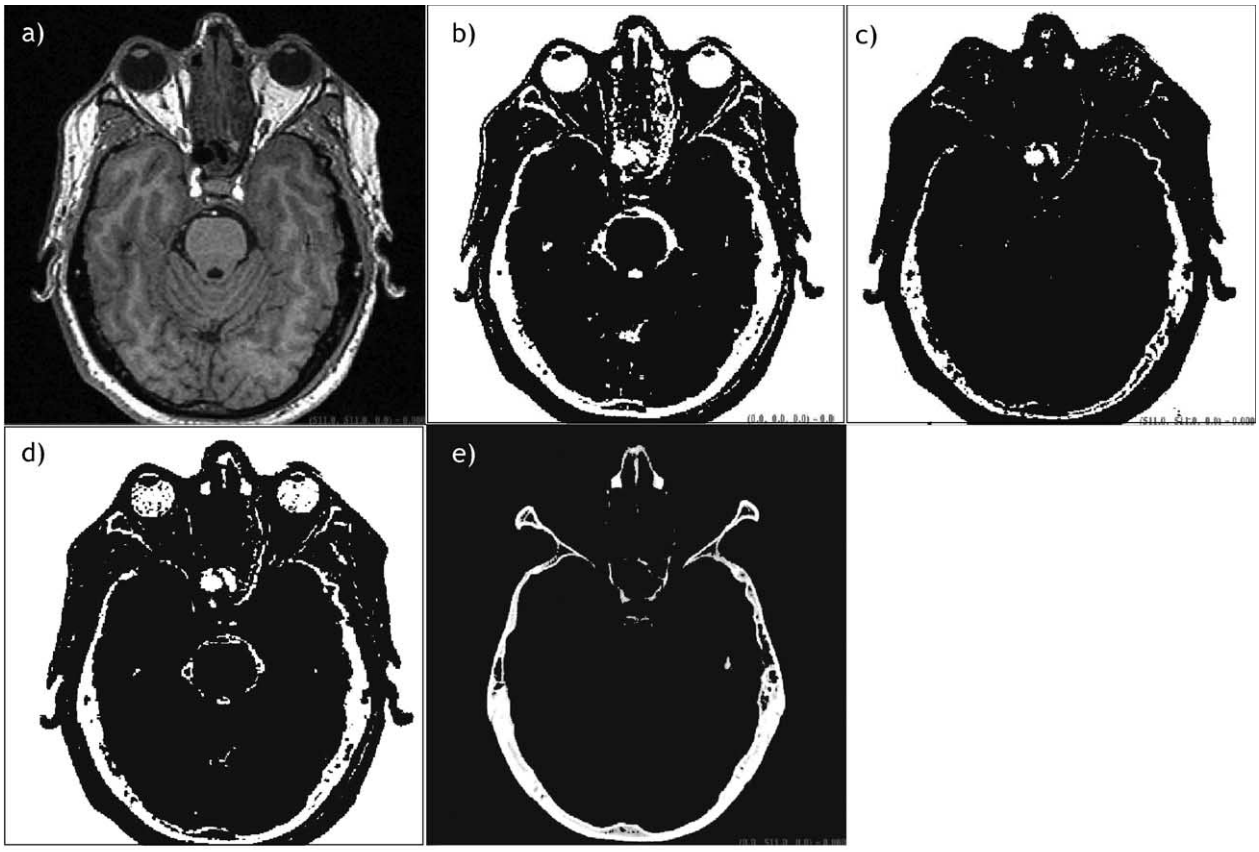

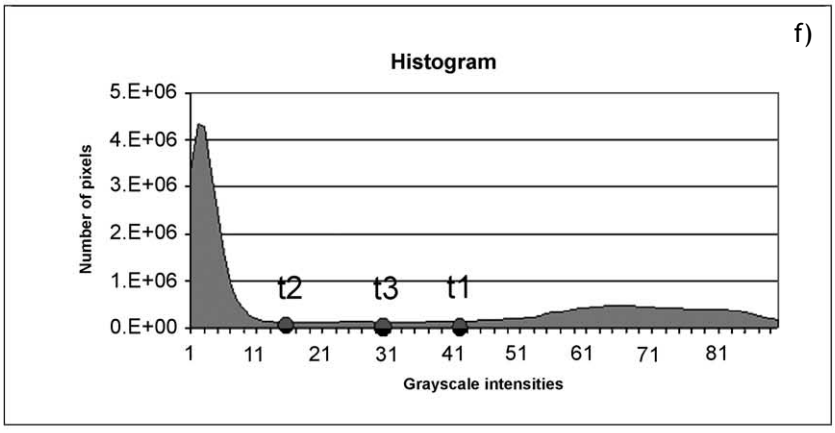

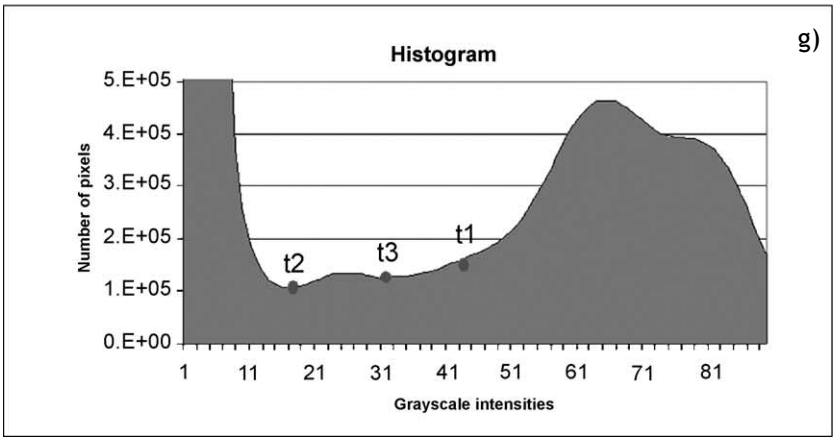

Fig. 3: Illustration of the segmentation results of the three Otsu thresholds.
a) MR image
b) MR image after application of the first Otsu threshold t1 and grayscale inversion,
c) MR image after application of the second Otsu threshold t2 and grayscale inversion,
d) MR image after application of the third Otsu threshold t3 and grayscale inversion. Although some air-cavities and cerebrospinal fluids are also segmented, their effect is not serious, because the algorithm looks only at voxels corresponding to segmented bone voxels in the CT, seen in (e).
f) Histogram of the MR image and g) close-up view on the histogram.

Hounsfield units (Fig. 2c). The isolated bone volume of bone structures is labeled SCT .

Bone structures in the MR image are segmented using a custom segmentation algorithm, yielding a subvolume S_{MR1} (Fig. 2d).

The bone volume S_{CT} is mapped onto the MR dataset, and the resulting MR subvolume is labeled S_{MR2}.

S_{MR2} is then color-coded as follows: Voxels that belong to S_{MR2} and to S_{MR1} are classified as 'safe', representing a high registration accuracy, and are colored green. Voxels that belong to S_{MR2} but not to S_{MR1} are classified as 'unsafe', representing a local low registration accuracy and are colored red.

A fused CT-MR image is synthesized by overlaying the color-coded subvolume S_{MR2} onto the original MR (Fig. 2e).

The algorithm is implemented in C++, using the open source Insight Segmentation and Registration Toolkit Library for medical image processing.

Segmentation of bone structures in MR

In step 3 of the above-described CT-MR registration assessment, a custom algorithm for bone segmentation in MR is employed. Segmenting bone in MR (T1-weighted sequence) is difficult due to its low signal intensity and the difficulty in distinguishing bone from other low signal intensity classes such as air and cerebrospinal fluids.

To find an adequate threshold to separate bone from soft tissue, we employed a triple application of Otsu's nonparametric, automatic threshold selection method [11], which is used to separate objects from their background. Otsu's algorithm computes the optimal threshold that separates the object class from the background class by maximizing the between-class variance. In MR images, there are more than two main classes (air, cerebrospinal fluids, bone, gray matter, white matter, muscle, and fat). A first application of Otsu's algorithm on the MR image, yields a threshold T1, which roughly separates the low-signal intensity classes from the high-signal intensity classes, see Figure 3b. The low-signal classes include air, bone, cerebrospinal fluids, and some soft tissues, while the high-signal class represents various other soft tissues. Thus, this threshold is not sufficient for bone segmentation from soft tissues, but it is used to remove the higher intensity classes from the MR image. The resulting image is processed a second time by Otsu's algorithm yielding a new threshold T2, which separates the lowest intensity classes from the rest, but which does not provide an satisfactory threshold for bone either (Figure 3c). Finally, the Otsu algorithm is applied a third time, this time considering only voxels with intensities between T1 and T2. The new threshold T3 separates the voxels in the T1—T2 range into a low- and a high-intensity class. The computed threshold T3 offers a fair segmentation threshold for bone (Fig. 3d).

The drawback of this simple thresholding method is that some undesired smaller areas with air cavities, cerebrospinal fluids, and the background are also segmented. However, the effect on the registration assessment algorithm is small, since the assessment in this algorithm is not performed on the whole image volume, but only on the subvolume representing the skull S_{MR2}. In fact, it can be shown that no single threshold can unambiguously separate bone from other structures in MR of the head area. Because voxels have a finite size, partial-volume effects occur where voxels contain a mixture of two materials, leading to segmentation errors for voxels at the border between bone and soft tissues. Segmentation problems also exist for thin bone structures.

Results

Validation with simulated CT-MR data

Given the fact that there is a lack of real ground-truth in normal MR data, we employed simulated MR data (T1-weighted) provided by the MR-simulator from the McGill University, Montreal, Canada [12] to evaluate the presented bone segmentation algorithm. The simulator provides complete, realistic MR volumes of the head at different noise levels and intensity inhomogenies. It also provides separate volumes of the main tissue classes that make up the anatomical model such as bone, background, cerebrospinal fluids, gray matter, and white matter. The bone tissue class was treated as the ground-truth for segmented bone. The percentage of the bone volume that was segmented by the algorithm was computed by the expression:

$$r_{bone} = \frac{S_{MR} \bigcap S_b}{S_b}$$

with S_{MR} representing the volume of segmented bone and S_b the a priori known bone volume, provided by the simulator. The value of r_{bone} is equal to one if S_b is fully contained in S_{MR}, and equal to zero if the two volumes do not overlap.

The bone segmentation algorithm was tested on simulated MR datasets with different levels of noise and intensity non-uniformity. For intensity

noise levels ranging from 0—7% and intensity non-uniformities from 0—20% of the full intensity scale, the r_{bone} values were above 98%, indicating that the algorithm is effective and stable for the mentioned levels of noise and intensity non-uniformity. For higher noise and intensity non-uniformity levels, which are uncommon, the Otsu-based segmentation algorithm fails. As explained in the methods section, the algorithm segments more than only pure bone. It also segments small areas of cerebrospinal fluids and air cavities, which represent false positive errors.

Evaluation with real CT-MR data

In addition to the evaluation on simulated data, the assessment algorithm was successfully applied on CT-MR image pairs from eight patients, which were registered using normalized mutual information [13]. However, due to the lack of ground-truth when using real data, the validation of the registration assessment result is difficult. The approach presented here was to evaluate the results on a set of CT-MR pairs with controlled misregistrations. Starting from a well-registered image pair, we translated the CT dataset first in the mediolateral direction and then in the anterioposterior direction by 3 mm. In the processed color-coded fused images shown in Figure 4, it is confirmed that the area of misregistration (red = 'unsafe' voxels) increases in the the lateral and anterioposterior directions by 3 mm, which is consistent with the first and second translations.

Another approach to evaluating the results of the registration assessment algorithm on real data is the following: A pair of CT and MR images was registered by mutual information and then processed by the registration assessment algorithm. A small 3-D subvolume (50x50x50 voxels) was then extracted from homologous locations of the CT and MR volumes. These subvolumes were then re-registered locally using mutual information and the subvolumes were re-processed by the registration assessment algo-

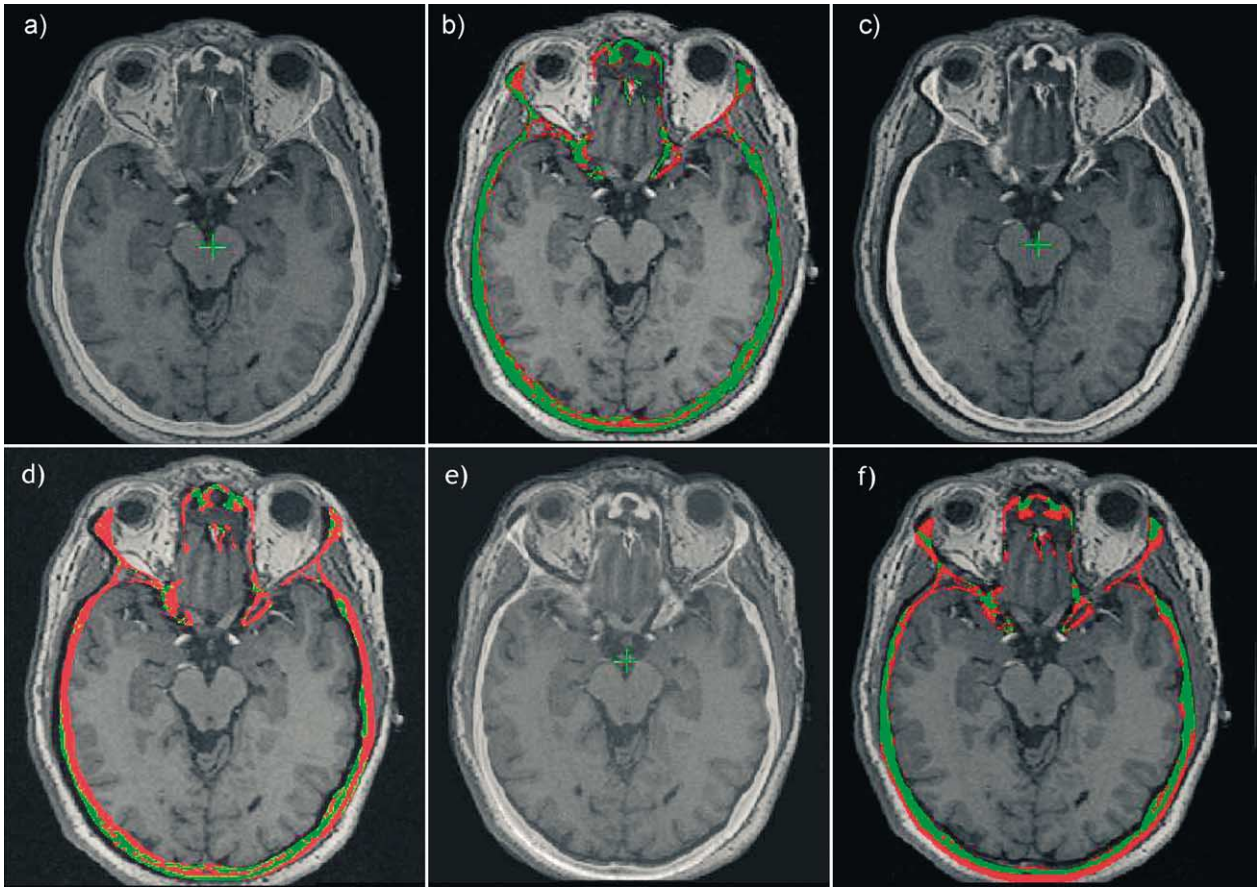

Fig. 4: The figure illustrates the benefit of the color-coded result of the registration assessment method. The first row shows conventionally fused datasets, where the CT has been overlaid on the MR. The second row shows a fused dataset with the overlaid color code. a) and b) show a well-registered image pair, c) and d) show an image pair with a purposely introduced mis-registration of 3 mm in mediolateral direction, e) and f) show an image pair with a purposely introduced mis-registration of 3 mm in anterioposterior direction. The color-code assessment result highlights bad (red) correspondences between the bone voxels in CT and MR images, that may otherwise pass unnoticed.

rithm. The assumption here was that registration performed on a small volume of interest would yield a better registration for that volume of interest than would a global registration performed on the whole volume. The expected improvement in registration accuracy is seen in the example provided in Fig. 5.

Conclusion

In several clinical cases, both a CT and an MR scan of the patient are necessary to understand the extent of the pathology. To relate the two complementary sources of information, the two datasets are usually co-registered and fused into a single display. However, as discussed in section 1, several reasons such as calibration and scaling errors, local minima in the optimization algorithm, and distortion can lead to local or global misregistrations. Visual assessment of the registration quality requires focused attention and the detection of small registration errors is difficult even if colored semi-transparent overlays are used to represent one modality on top of the other.

Although other authors have previously compared and evaluated the performance of different CT-MR registration techniques, our aim was to provide an automatic method to assess local registration errors for standard clinical use without the use of fiducials or landmarks. The registration assessment presented here is based on a correspondence analysis of bone structures in the original image only. Soft tissues are unsuitable for the correspondence analysis because they produce unspecific gray values in CT imaging. However, a well-registered hard tissue structure strengthens the reliability of the registration of other parts of the image. The presented method has the potential to reduce the risk induced by the unknowing use of misregistered CT-MR datasets in diagnostic or interventional applications.

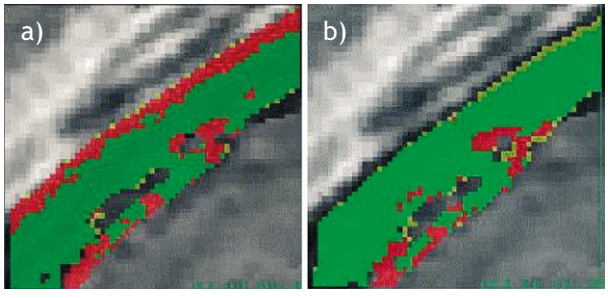

Fig. 5: a) shows a small 3-D sub-volume extracted from a larger registered CT-MR image pair. In the middle the color-coded overlay visualizes the registration assessment result for bone structures. In (b) the CT and MR sub-volumes have been re-registered to each other using a mutual information algorithm. The re-registered sub-volumes exhibit a strongly improved registration assessment result, the low-accuracy (red) region is greatly diminished.

For the segmentation of bone in the MR images, a custom method based on Otsu's automatic threshold selection method was used. On the basis of simulated MR data, we have shown that this method segments more than 98% of the bone for normal noise levels. However, it also segments some cerebrospinal fluids and air cavities, causing some correspondence errors between the CT and MR to not be detected. This error leads to an optimistic registration assessment and represents a limitation of any intensity-based assessment method, due to the low bone intensity and contrast in standard MR datasets. In the future, a more morphology-oriented and model/knowledge-based MR bone segmentation algorithm [14] could further reduce this error.

Acknowledgments

We would like to acknowledge Mrs. Spielvogel and Dr. Remonda from the Neuroradiology Department at the Inselspital Bern for providing the patient data and for the valuable discussions, Daniel Rückert, Department of Computing, Imperial College, UK [15] for providing the tool for rigid normalized mutual information registration, and the Swiss National Science Foundation and the CO-ME (http://www.co-me.ch) consortium for supporting the project.

References

1. Maintz JB, Viergever MA (1998) A survey of medical image registration. Med Image Anal; 2: 1—36.
2. West J, Fitzpatrick JM, Wang MY, et al. (1997) Comparison and evaluation of retrospective intermodality brain image registration techniques. J Comput Assist Tomogr; 21: 554—556.
3. Hawkes DJ (1998) Algorithms for radiological image registration and their clinical application, J Anat; 193 (Pt 3): 347—361.
4. Viola P, Wells WM (1997) Alignment by maximization of mutual information. International Journal of Computer Vision; 24 (2); 137—154.
5. Pluim JP, Maintz JB, Viergever MA (2000) Image registration by maximization of combined mutual information and gradient information. IEEE Trans Med Imaging; 19 (8): 809—814.
6. Hill DLG, Jarosz J Registration of MR and CT Images for Clinical Applications, in Book Medical Image Registration. CRC Press.
7. Maurer CR, et al. (2002) Sources of Error in Image Registration for Cranial Image-Guided Surgery, Advanced Techniques in Image-Guided Brain and Spine Surgery. New York: Thieme; 10—36.

8. Fitzpatrick JM, Hill DL, Shyr Y (1998) Visual assessment of the accuracy of retrospective registration of MR and CT images of the brain. IEEE Trans Med Imaging; 17 (4): 571—585.
9. Woods RP (2000) Validation of Registration Accuracy, Handbook of Medical Imaging, Processing and Analysis. Ed. Bankman, I. N., Academic Press.
10. National Library of Medicine Insight Segmentation and Registration Toolkit (ITK). ITK is an open-source software system to support the Visible Human Project. http://www.itk.org
11. Otsu N (1979) A threshold selection method from Gray-Level Histograms. IEEE Trans on Systems, Man, and Cybernetics; SMC-9(1): 62—66.
12. McConnell Brain Imaging Centre Montreal Neurological Institute, McGill University, Canada, http://www.bic.mni.mcgill.ca/brainweb/.
13. Studholme C, Hill DL, Hawkes DJ (1996) Automated 3-D registration of MR and CT images of the head. Med Image Anal; 1(2): 163—175.
14. Dogdas B, Shattuck DW, Leahy RM (2002) Segmentation of the skull in 3D human MR images using mathematical morphology. Proc SPIE Medical Imaging Conf; 4684: 1553—1562.
15. Rueckert D, Hawkes DJ (1999) 3D analysis: Registration of biomedical images. In:Baldock R, Graham J (eds) Image Processing and Analysis—A Practical Approach, Oxford University Press.

Correspondence address:

Ion P. Pappas, Dr. sc. tech. ETHZ
MEM Research Center for Orthopaedic Surgery
Institute for Surgical Technology and Biomechanics
University of Bern
Murtenstrasse 35, P.O. Box 8354
3001 Bern, Switzerland
phone: +41 31 632 3565
fax: +41 31 632 4951
email: ion.pappas@MEMcenter.unibe.ch